Heliyon 10 (2024) e27162

Contents lists available at ScienceDirect

Heliyon

journal homepage: www.cell.com/heliyon

Research article

A PANoptosis pattern to predict prognosis and immunotherapy response in head and neck squamous cell carcinoma

Feng Gao [a], Minghuan Zhang [b], Zhenguang Ying [b], Wanqiu Li [b], Desheng Lu [b], Xia Wang [b,*], Ou Sha [a,**]

[a] School of Dentistry, Institute of Stomatological Research, Shenzhen University Medical School, Shenzhen University, Shenzhen, China
[b] Shenzhen University Medical School, Shenzhen University, Shenzhen, China

ARTICLE INFO

Keywords:
PANoptosis
Head and neck squamous cell carcinoma
Cancer immunotherapy
Non-apoptotic cell death
Pathological malignancy

ABSTRACT

Individuals diagnosed with head and neck squamous cell carcinoma (HNSCC) experience a significant occurrence rate and are susceptible to premature spreading, resulting in a bleak outlook. Therapeutic approaches, such as chemotherapy, targeted therapy, and immunotherapy, may exhibit primary and acquired resistance during the advanced phases of HNSCC. There is currently no viable solution to tackle this issue. PANoptosis—a type of non-apoptotic cell death—is a recently identified mechanism of cellular demise that entails communication and synchronization among thermal apoptosis, apoptosis, and necrosis mechanisms. However, the extent to which PANoptosis-associated genes (PRG) contribute to the forecast and immune reaction of HNSCC remains mostly undisclosed. The present study aimed to thoroughly analyze the potential importance of PRG in HNSCC and report our discoveries. We systematically analyzed 19 PRG from previous studies and clinical data from HNSCC patients to establish a PAN-related signature and assess its prognostic, predictive potential. Afterward, the patient information was separated into two gene patterns that corresponded to each other, and the analysis focused on the connection between patient prognosis, immune status, and cancer immunotherapy. The PAN score was found to correlate with survival rates, immune systems, and cancer-related pathways. We then validated the malignant role of CD27 among them in HNSCC. In summary, we demonstrated the effectiveness of PAN.Score-based molecular clustering and prognostic features in predicting the outcome of HNSCC. The discovery we made could enhance our comprehension of the significance of PAN.Score in HNSCC and facilitate the development of more effective treatment approaches.

1. Introduction

Head and neck malignancies are classified as the sixth most prevalent form of cancer globally, with approximately 90% of cases being head and neck squamous cell carcinomas (HNSCC) [1,2]. HNSCC is recognized for its elevated occurrence of metastasis to cervical lymph nodes, heightened invasiveness, and tendency to recur, ultimately resulting in an unfavorable prognosis [3]. HNSCC is usually treated with surgical removal, chemotherapy, radiotherapy, immunotherapy, or a combination of these approaches. However,

* Corresponding author.
** Corresponding author.
E-mail addresses: xia.wang@szu.edu.cn (X. Wang), shaou@szu.edu.cn (O. Sha).

https://doi.org/10.1016/j.heliyon.2024.e27162
Received 13 November 2023; Received in revised form 20 February 2024; Accepted 26 February 2024
Available online 27 February 2024

the limited effectiveness of these treatments is attributed to the tumor's heterogeneity [4,5]. Fortunately, the survival rate of HNSCC individuals has considerably enhanced compared to previous times because of the progress in chemotherapy and targeted medications. Several improvements have been made in cancer management over the past few years because of the progress in tumor immunotherapy and immune checkpoint blockers. Studies have demonstrated that immune checkpoint therapy, which focuses on PD1/PD-L1, greatly extends the lifespan of individuals diagnosed with advanced HNSCC [6,7]. Studies have demonstrated that patients with different forms of cancer, including HNSCC, may experience primary resistance to PD1/PD-L1 inhibitors, with rates reaching as high as 60% [8,9].

HNSCC is a cancer that heavily relies on programmed cell death [10]. However, traditional treatments often lead to problems, such as restricted toxicity and resistance to therapy. PANoptosis is an innovative type of programmed cell death that occurs when programmed death pathways combine and work together inside cells. The concept of PANoptosis, which has recently been uncovered, emphasizes the intercommunication and synchronization among pyroptosis, apoptosis, and necroptosis [11]. Inducing PANoptosis can trigger the release of cytokines from tumor cells, which in turn stimulate an immune response. These cytokines can activate the body's immune system to target and eliminate tumor cells [12]. Moreover, PANoptosis can effectively prevent the development of drug resistance in tumor cells [13]. The findings indicate that PANoptosis can be an innovative approach for treating head and neck cancer, offering potential therapeutic benefits.

Extensive functional evaluations of PANoptosis have been conducted in vitro and in vivo mouse models. Tumorigenesis is suppressed by IRF1-induced PANoptosis in a colorectal cancer mouse model [14]. In a mouse melanoma model, Z-DNA binding protein 1 (ZBP1) can kill cancer cells by activating PANoptosis [15]. In the meantime, in cancerous cell lines of humans, PANoptosis can be triggered by simultaneously treating with TNF-α and IFN-γ [16]. Despite these progressions, there is still a lack of comprehension concerning the predictive effect of PANoptosis on the overall survival (OS) of individuals with different forms of cancer.

Cancer immunotherapy has witnessed a surge of interest in non-apoptotic cell death, particularly PANoptosis [17]. A recently identified form of cell death known as PANoptosis includes the concurrent activation of several pathways, including apoptosis, necroptosis, and pyroptosis. The implications of this coordinated and comprehensive response to cellular stress extend to a number of pathological conditions, including cancer. PANoptosis is a cancer immunotherapy that holds a lot of promise for boosting the immune system's ability to fight tumors. Through the induction of PANoptosis in cancer cells, the immune system is notified by the release of danger-associated molecular patterns and pro-inflammatory cytokines that act as "alarms". As a result, these signals help to mobilize and energize immune cells, thereby fostering an immune response against tumors.

Researchers have uncovered the suppressive effect of PANoptosis on the development of tumors in various types of cancer, offering further insights for exploring biomarkers and treatment targets for patients [13,15,17,18]. However, the specific influence of PANoptosis on the outcome of HNSCC remains unknown. A few studies have described PANoptosis-related patterns or identified PRG signatures in HNSCC. Gaining insight into the fundamental processes of PANoptosis may provide new opportunities for advancing HNSCC immunotherapy by exploring alternative approaches.

HNSCC represents a significant global health burden, with rising prevalence and mortality rates. Despite advances in treatment, challenges persist, particularly in the context of immunotherapy, where response rates vary widely, underscoring the need for innovative treatment strategies and predictive tools like PAN.Score. After a comprehensive analysis of the expression of PANoptosis genes, we identified two distinct PANoptosis patterns (PAN.Clusters) among HNSCC individuals. Both PANoptosis pattern possesses unique molecular, clinical, and immunological attributes. Furthermore, we established PAN.Score, which is effective in prognosis prediction and prediction of treatment response in HNSCC. Finally, the malignant role of CD27 in HNSCC was validated among them. In summary, we demonstrated the effectiveness of PAN score-based molecular clustering and prognostic features in predicting the outcome of HNSCC. Our discovery could enhance our comprehension of the significance of PAN score in HNSCC and facilitate the development of more efficient treatment approaches. This study aims to explore the prognostic value of PAN.Score in HNSCC and its potential to predict immunotherapy response. We hypothesize that PAN.Score can serve as a reliable biomarker, aiding in the personalized treatment of HNSCC patients.

2. Materials and methods

2.1. Collecting and preparing data

The TCGA (519 samples) [19] and GEO (GSE41613 (97 samples), GSE42743 (103 samples), and GSE65858 (270 samples) provided comprehensive clinicopathological annotation and genomic data for HNSCC. Gain entry to the Gene Expression Omnibus (GEO) of the National Library of Medicine [20].

Raw data was generated from the GEO database using the Affymetrix and Illumina platforms. Exclusion was done for patients who did not have sufficient OS data. For background correction and normalization, the RMA algorithm, which is strong and involves multiple chips, was utilized. RNA sequencing data and methylation data were provided by the TCGA database. Transcripts per kilobase (TPM) values were obtained by converting the Fragments per kilobase (FPKM) values using signal intensities comparable to RMA processing [21].

2.2. Establishment of PAN.Cluster

For subsequent clustering, a collection of 19 PAN-associated genes that are associated with non-apoptotic cell death was acquired [22]. The list of genes includes CASP8, FADD, CASP6, NLRP3, TAB2, TAB3, PSTPIP2, TNFAIP3, CASP7, IRF1, PARP1, GSDMD, MLKL,

RIPK1, RIPK3, AIM2, ZBP1, CASP1 and TRADD. Patients with varying gene expression profiles related to PANoptosis in HNSCC were categorized using 'Pam' methodology deciding the best clusting numbers based on these 19 PAN-associated genes, identifying PAN-related patterns utilizing the R package 'ConsensusClusterPlus' [23].

2.3. Establishment of PAN.Score

The analysis utilized the 'limma' package in R to identify genes that showed differential expression with a log fold change exceeding 1 and a p-value below 0.05. For this objective, a grand total of 145 genes were examined. Subsequently, the prognosis of PAN was further investigated by performing a one-way Cox regression analysis using the 'survival' package in R language, aiming to identify genes associated with it (with a significance level of $P < 0.05$). A total of 21 genes were successfully recognized. Afterward, we employed a survival machine learning algorithm with the R 'randomSurvivalForest' package to discover more PAN-related genes that possess prognostic potential (with variable relative importance exceeding 0.2). This screening process successfully identified a total of 3 genes. The PAN.Score was generated by combining PAN genes linked to prognosis and their regression coefficients estimated in the Lasso regression analysis. In the heat map, asterisks (*) indicate levels of statistical significance, with $*p < 0.05$, $**p < 0.01$, and $***p < 0.001$, providing a clear indication of the robustness of the observed associations.

2.4. Validation of the efficacy of PAN.Score

The PAN.Score was computed for 519 individuals in the TCGA-HNSCC dataset. Afterward, the individuals were classified into high and low PAN.Score groups according to the P value of the best threshold. We analyzed the correlation between OS and PAN.Score by utilizing Kaplan-Meier curves. The timeROC was used to validate the prognostic prediction efficiency and accuracy of PAN.Score at 1, 3, and 5 years.

2.5. Genomic alteration

Somatic mutations were gathered using TCGA datasets. The analysis of somatic mutations was performed using the 'maftools' package [24].

2.6. Evaluation of the TME immunological profile

The ESTIMATE method utilizes immune scores, stromal scores, and estimated scores to assess the quantity of immune cells and the level of stromal cell infiltration. To investigate immune infiltrating cells in HNSCC, we employed the web server Tumor Immune Estimation Resource 2.0 (TIMER2.0). The GSVA tool was employed to analyze genomic variance in the R package, in conjunction with single sample genomic enrichment analysis, to generate an enrichment score that reflects the extent of infiltration by 28 immune cells. This score is determined based on their associated characteristics (ssGSEA) [25,26].

2.7. Functional annotation

We acquired various collections of genes from the MSigDB database [27], KEGG, and Gene Ontology (GO). Gene set enrichment analysis (GSEA) and genomic variation analysis (GSVA) were conducted using the R packages clusterProfiler [28] and GSVA [29].

2.8. Prediction of drug response

The prediction of drug susceptibility was made using the pharmacogenomic data obtained from Genomics of Drug Sensitivity in Cancer (GDSC). The drug response was calculated by using the oncoPredict R package to determine drug susceptibility [30].

2.9. Cell experiments

2.9.1. Lentiviral vector construction and infection

SCC15 (HNSC cell line) was purchased from the American Type Culture Collection (ATCC), and the cells were cultured as described in Ref. [31]. SCC15 cells achieved high transfection efficiency and stable knockdown CD27 expression using lentiviral-containing green fluorescent protein (GFP) (Gene Copoeia Company, Guangzhou, China). Afterward, the previously mentioned lentiviral vectors were employed for infecting SCC15 cells. Initially, 1×10^6 SCC15 cells were placed in a six-well cell plate and allowed to grow for an additional 12 h until they achieved a 70% confluence. Afterward, lentiviral vectors were added to the infection medium at a ratio of 20 units per cell. The establishment of two groups was done in the following manner: shCD27 (the group with knockdown expression of CD27) and control (the group with control vector). After 24 h of incubation, the plates were subjected to fresh media devoid of any viruses. After three days, the lentivirus density containing GFP was measured in order to evaluate the effectiveness of the infection. Then the total RNA was isolated by TRIzol reagent (ComWin Biotech Co, Suzhou, China). Single-stranded cDNA was generated by a Super RT cDNA Synthesis kit (ComWin Biotech). The qRT-PCR was performed using an ULtraSYBR Mixture kit (Low ROX) according to the manufacturer's protocol. The primer sequences are as follows. CD27, forward 5′ - TGTGATCCTTGCATACCGG-3′, reverse 5′ - ACGAGAAGACCAGAGTTACAG-3′; and GAPDH, forward 5′ - TCAAGATCATCAGCAATGCC-3′, reverse 5′ -

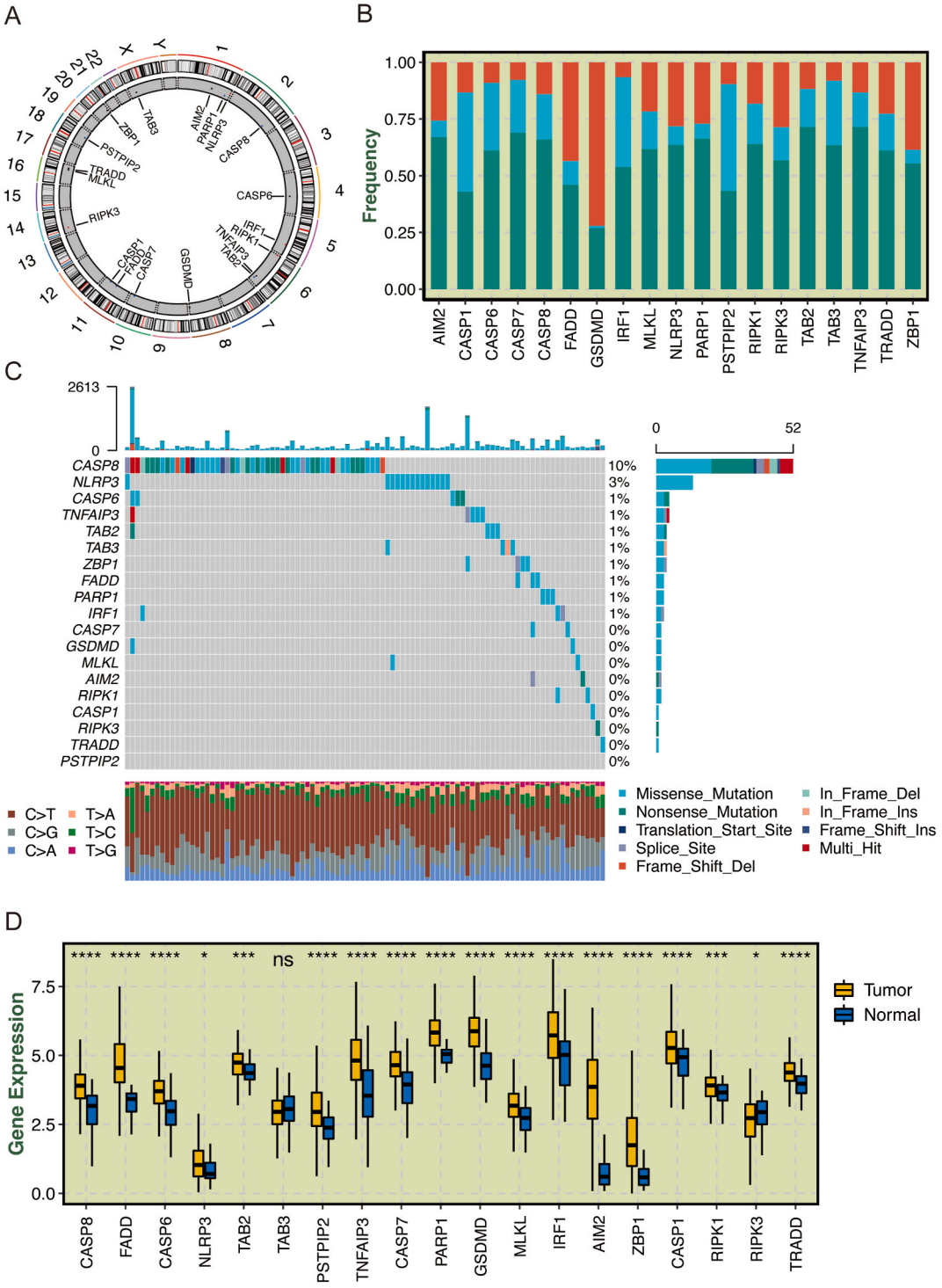

Fig. 1. Characteristics of PAN-associated genes in HNSCC. (A) The distribution of 19 PRGs on chromosomes (B) Bar graphs showing the frequency of CNV of 19 genes in TCGA-HNSCC (C) The mutation frequency of 19 genes in TCGA-HNSCC cohort. (D) Box plots show the expression distribution of 19 genes between normal and tumor samples in TCGA-HNSCC cohort. *p < 0.05; ***p < 0.005, ****p < 0.001.

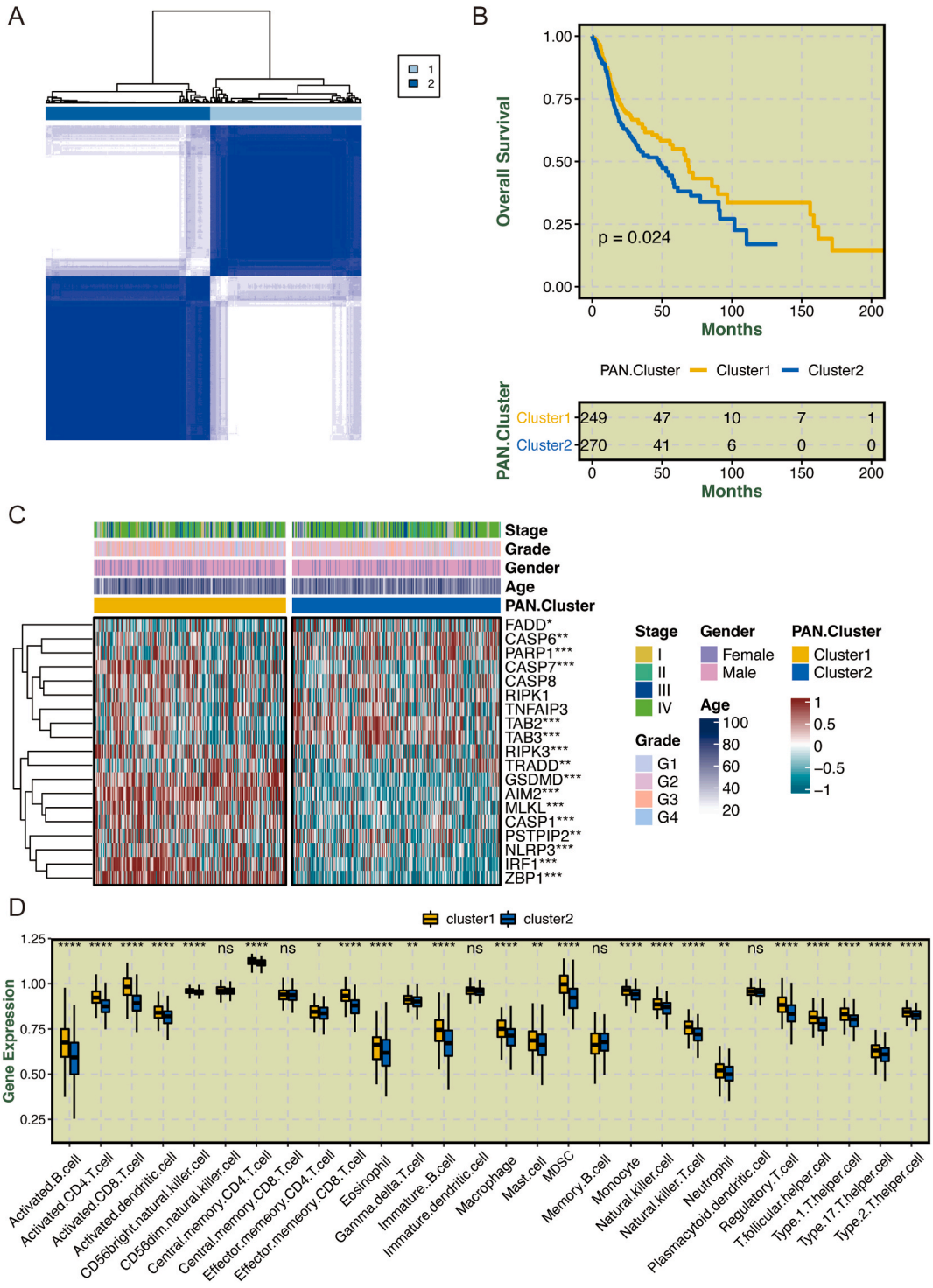

Fig. 2. Establishment of PAN. Cluster (TCGA-HNSCC). (A) Two PAN. Clusters were defined using consensus clustering analyses. (B) Kaplan-Meier curve showing the correlation between PAN. Cluster and OS (C) Heatmaps showed the relationship between PAN. Clusters and clinical features in HNSCC patients (D) ssGSEA investigated the differences in immune cell infiltration between two clusters. *p < 0.05; **p < 0.01, ***p < 0.005, ****p < 0.001.

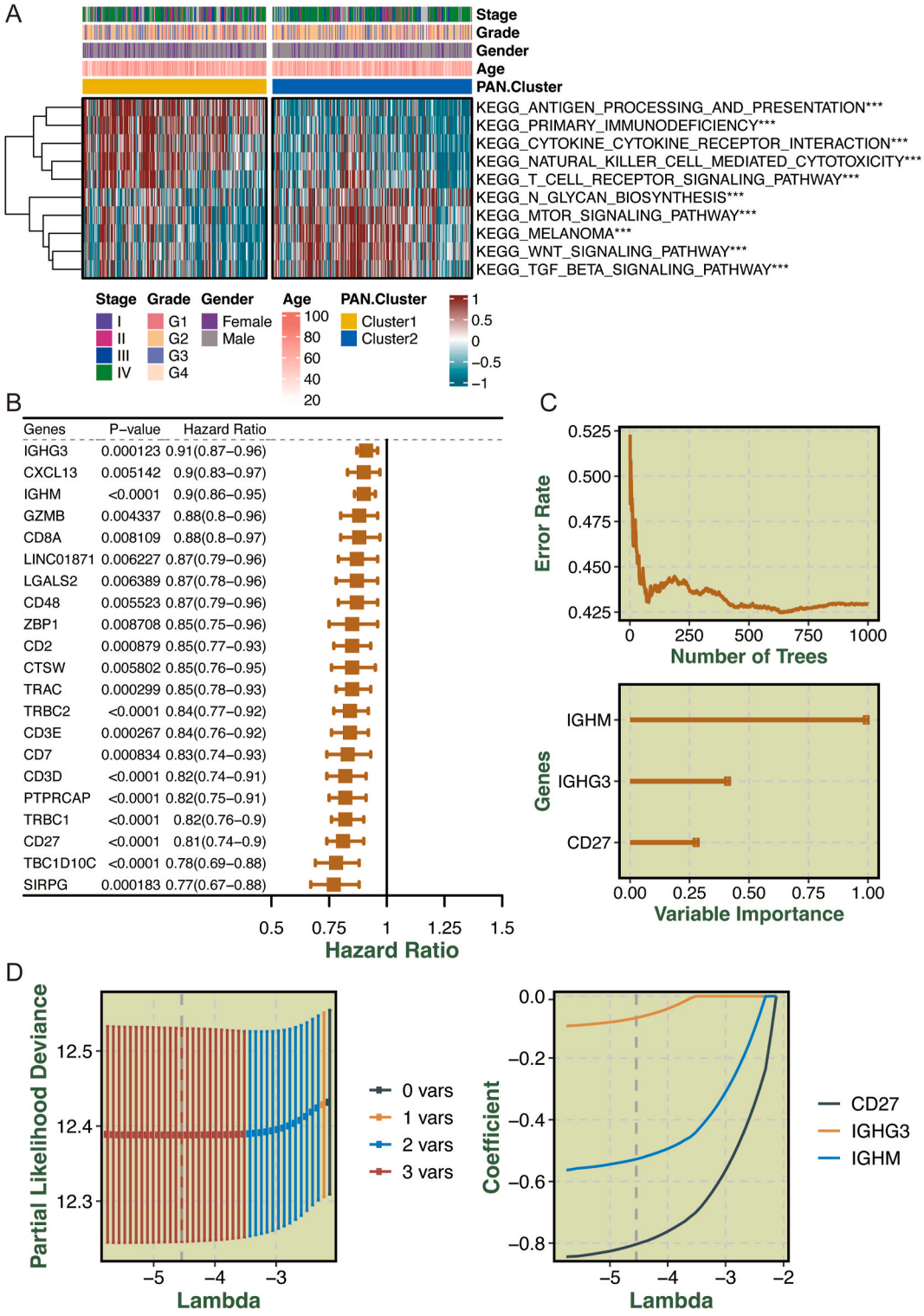

Fig. 3. Establishment of PAN.Score(TCGA-HNSCC). (A) The association between GSVA-KEGG pathways and PAN. Cluster (B) Forest plot of univariate Cox analysis showing 21 prognosis-related factors for PAN. Cluster (C)Machine learning method for survival random forest to further screen PAN. Cluster. (D) Lasso regression method to calculate PAN.Score. ***p < 0.005.

CGATACCAAAGTTGTCATGGA-3′. Quantification was performed using the ΔΔCt method, and the data were normalized to GAPDH (acting as control).

2.9.2. MTT assay

In order to evaluate cell proliferation, the transfected cells were placed into 96-well plates. After incubating for 24, 48, and 72 h at a temperature of 37 °C and a CO_2 concentration of 5%, a solution of 20 L of MTT (Sigma, USA) was added to each well. Afterward, every well was cultured for one more hour. The microplate reader from Molecular Devices in Sunnyvale, CA was utilized to determine the OD value at a wavelength of 490 nm.

2.9.3. Detection of plate clones

In order to evaluate the ability of the transfected cells to produce colonies, 1000 cells were evenly distributed on every plate placed in 60 mm culture dishes. After a culture period of 10 days, the cells were subjected to treatment with a 10% neutral buffer formalin fixative and then stained with a crystal violet solution (Beyotime, China). We captured images and tallied the settlements.

2.9.4. Scratch migration assay

To evaluate cell migration, 6 well plates were inoculated with transfected cells. After 24 h of cell culture, a pipette tip was used to create a straight cut in each well. Subsequently, the cells were grown in a culture medium with 2% FBS, while being subjected to 5% CO_2 at a temperature of 37 °C. Wound closure assessment was performed after 24 and 48 h using a microscope (OLYMPUS, Tokyo, Japan) with a 4 × magnification [32].

3. Results

3.1. Features of PANoptosis-related genes in HNSCC

Information regarding gene expression in HNSCC patients was acquired from the TCGA database, and features of 19 PRGs were illustrated. Fig. 1A illustrates the distribution of PRGs on chromosomes. Fig. 1B shows bar graphs representing the frequency of CNV gain (red), loss (blue), and non-CNV (green) in 19 PRGs. The mutation frequency of 19 PRGs in HNSCC patients from the TCGA cohort (Fig. 1C). Fig. 1C displays the frequency of mutations in 19 PRGs in TCGA cohort patients with HNSCC. Among the 19 PRGs, 17 genes displayed elevated expression in the tumor samples, whereas the RIPK3, demonstrated reduced expression in the tumor samples ($P < 0.05$), without any significant change observed in TAB3 (Fig. 1D). Also, we correlated the expression profiles of PRGs with their promoter methylation status (Fig. S1).

3.2. The process of constructing PAN.Cluster in HNSCC

To examine the association between the PAN genes and their predictive significance, we divided HNSCC patients into Cluster 1 and Cluster 2 (Fig. 2A). The consensus CDF generated by ConsensusClusterPlus has proved the two clusters are the optimal number of classifications shown in Fig. S4. Fig. S2 depicts the relationship between PAN. Cluster and PRGs in HNSCC patients. Based on Fig. 2B, the cluster1 group had a notably longer survival time than the cluster2 group ($P = 0.024$). In HNSCC patients, Fig. 2C exhibits the association between PAN. Cluster, clinical characteristics, and PAN gene expression. Tumor infiltration and lymph node metastasis were associated with PAN. Cluster ($P < 0.05$).

We performed a ssGSEA analysis to assess the difference in immune cell infiltration between the two clusters, indicating that cluster1 exhibited higher levels of immune cell infiltration. Fig. 2D reveals the presence of activated immune cells of various classifications. Also, Fig. S3 depicts the relationship between PAN. Cluster and contribution of different cell death type-specific responses in HNSCC patients [33,34].

3.3. Establishment of PAN.Score

The GSEA analysis revealed that people with the PAN. Cluster 1 signature in HNSCC exhibited increased activity in various essential pathways related to the immune system, including activated T-cell pathways and other pathways.

To anticipate the signaling pathways linked to PAN. Cluster, we performed GSVA-KEGG investigations, including enrichment of antigen processing and presentation, primary immunodeficiency, cytokine-cytokine receptor interaction, natural killer cell-mediated cytotoxicity, and T cell receptor signaling pathways in HNSCC (Fig. 3A).

We performed univariate Cox regression analysis to discover more PAN. Cluster-related prognostic genes (with a P value less than 0.05). The analysis revealed 21 genes that may hold prognostic importance for HNSCC patients (Fig. 3B). Fig. 3C illustrates a forest plot that was generated to exhibit the prognostic hazard ratio of each gene. To summarize, the Lasso regression analysis was used to calculate fresh scores, considering the estimated regression coefficients of the prognostic and PAN. Cluster-associated genes (Fig. 3D). The PAN.Score signature for prognosis was determined as:

$$-0.5277*IGHM + -0.07*IGHG3 + -0.8034*CD27$$

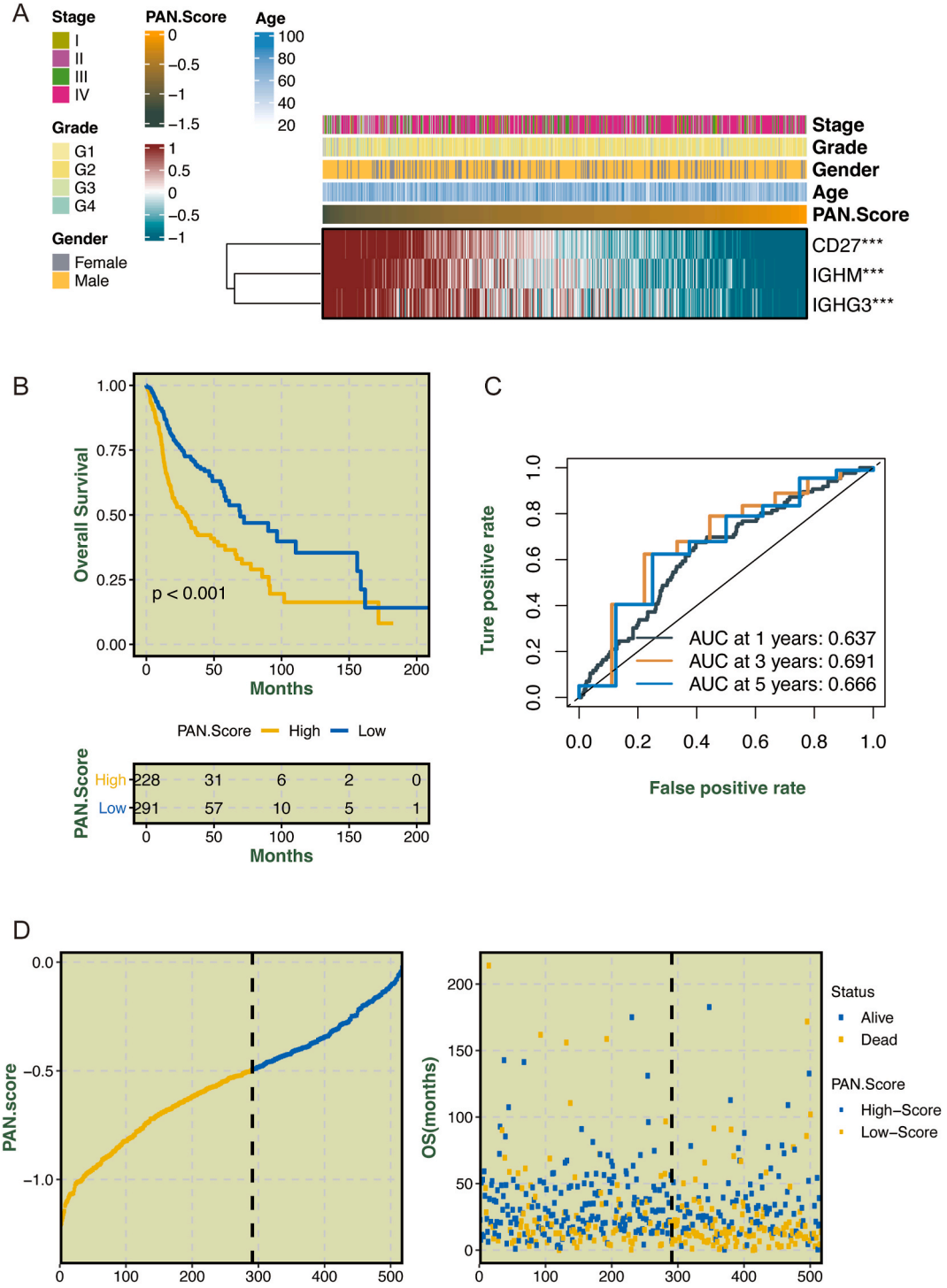

Fig. 4. Construction of the prognostic potential of PAN.Score. (A) Heat map showed the clinical features associated with the 3 PANoptosis genes in PAN.Score. (B) The Kaplan-Meier curve showed that patients with high PAN.Score group had a worse prognosis. (C) The AUC for 1-, 3- and 5-year survival were 0.637, 0.691, and 0.666, respectively (D) Risk score and survival outcome of each case. ***$p < 0.005$.

3.4. Prognostic potential of PAN.Score

The heat map (Fig. 4A) displayed the correlated clinical characteristics with PAN.Score genes, whereas the plotted KM curve (Fig. 4B) demonstrated the disparities in survival between the two groups. The chance of survival was significantly lower in the high-PAN.Score group than the low-PAN.Score group ($P < 0.001$). ROC curves were generated to assess the predictive precision of the risk score, resulting in AUCs of 0.637, 0.691, and 0.666 for 1-, 3-, and 5-year survival, respectively (Fig. 4C). Furthermore, patients were classified into high- and low-risk groups according to their risk scores, demonstrating higher mortality rates among patients with elevated risk scores (Fig. 4D). This finding suggests that our PAN.Score has prognostic significance.

Both single-variable and multiple-variable analyses showed that the PAN.Score independently influenced the prognosis of HNSCC patients (Fig. 5A). The accuracy of the nomogram prediction was evaluated using a calibration graph (Fig. 5B). The calibration

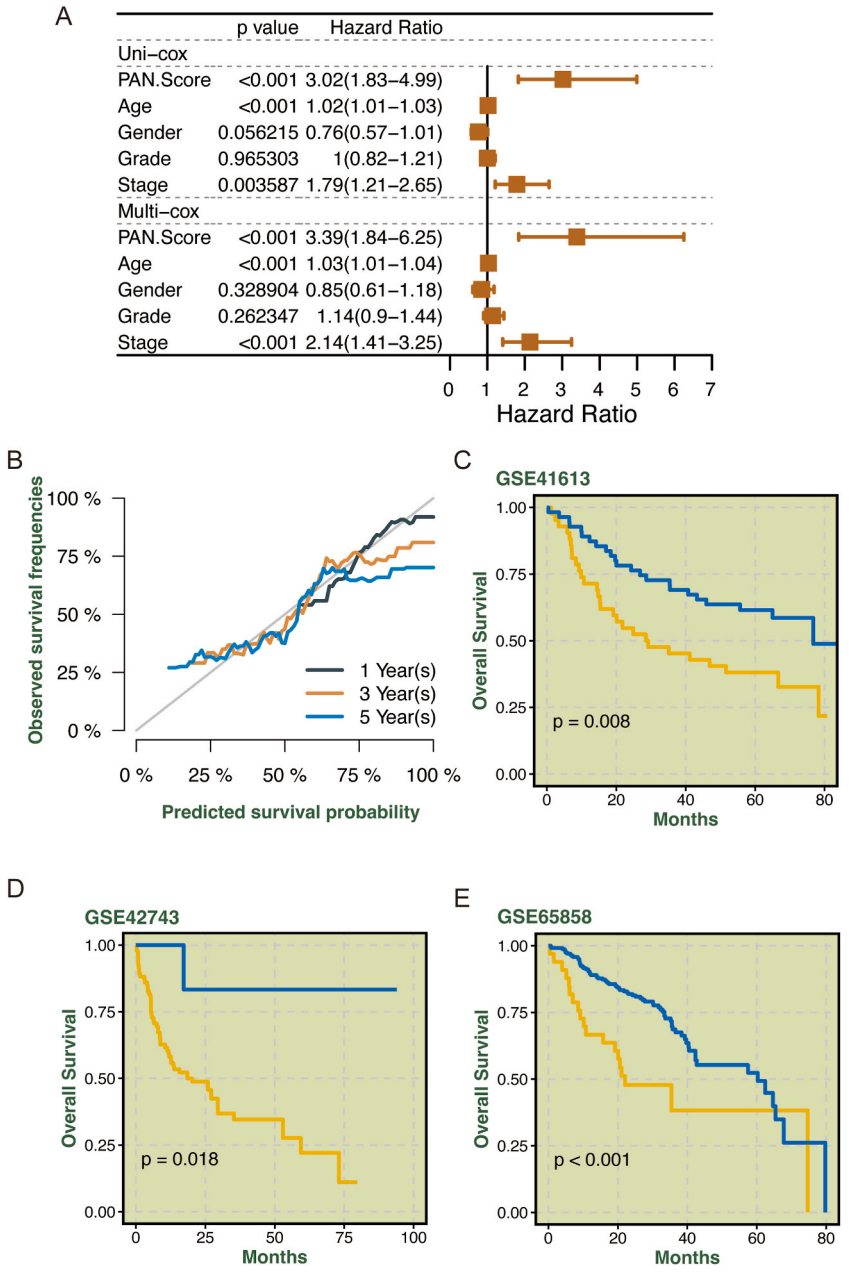

Fig. 5. Validation of the prognostic potential of PAN.Score. (A) Forest plots for univariate and multivariate cox regression based on the TCGA dataset of PAN.Score (B) Calibration graphs investigated that the actual survival rates of HNSCC patients were close to the survival rates. (C–E) The Kaplan-Meier curves were used to evaluate the efficiency of the risk score in predicting patient survival in GSE41613 (C), GSE42743 (D), and GSE65858 (E) datasets.

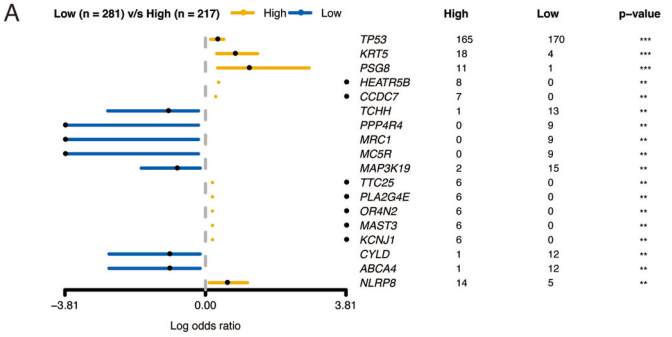

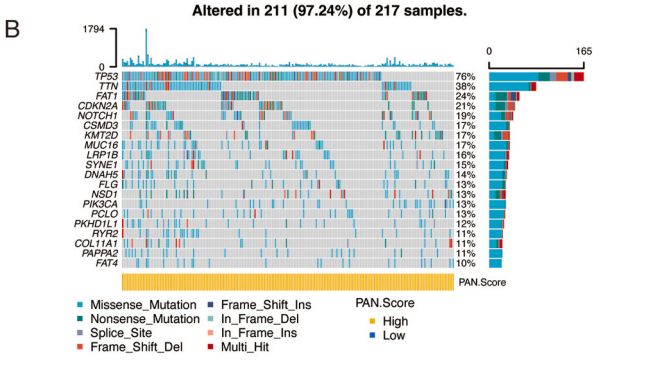

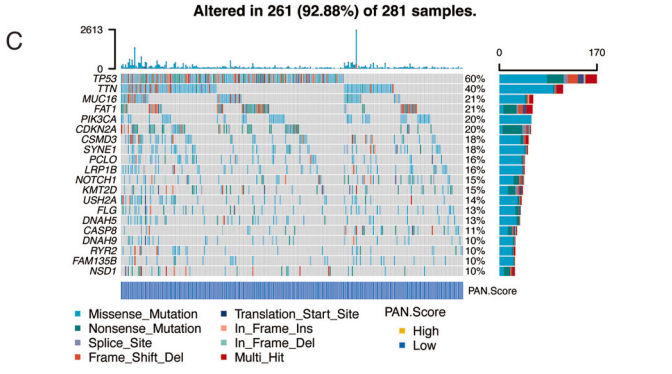

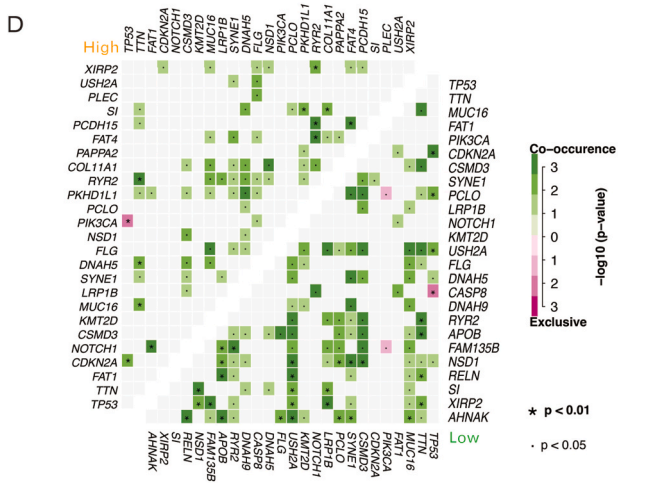

(caption on next page)

Fig. 6. Genomic alterations associated with PAN.Score in HNSCC samples. (A) Forest plot showing the results of somatic mutation difference analysis between high and low groups of PAN.Score. (B–C) Oncoplot of somatic mutations in HNSCCs between high and low PAN.Score groups. (D) The heatmap presents the somatic interaction of HNSCCs between PAN.Score high and low groups. *$p < 0.05$.

graphs—illustrating the differences in predicted survival probabilities by the nomogram and the real survival probabilities of HNSCC patients—demonstrated a strong similarity between the predicted and actual survival probabilities (Fig. 5B), indicating that the nomogram model accurately forecasted the survival of HNSCC patients. Based on the findings from three distinct validation cohorts (GSE41613, GSE42743, and GSE65858), the risk score was determined to be a dependable indicator of patient survival. This conclusion was supported by the results obtained from these cohorts, with GSE41613 showing a significant correlation (Fig. 5C, $P = 0.008$), GSE42743 demonstrating a notable association (Fig. 5D, $P = 0.018$), and GSE65858 displaying a highly significant relationship (Fig. 5E, $P < 0.001$).

3.5. Somatic alterations associated with PAN.Score in TCGA-HNSCC

The mutation frequency ratios between the high- and low-PAN.Score groups were compared using Fisher's exact test, and the results were sorted according to the ascending p-values. In Fig. 6A, the high PAN.Score group had a higher occurrence of PSG8 and KRT5 mutations than the low PAN.Score group. To ascertain the correlation between PAN.Score and somatic mutations, we conducted the Genomic Identification of Important Targets in Cancer (GISTIC) analysis. The examination uncovered that high- or low-PAN.Score HNSCC patients exhibited distinct genetic mutations, such as TP53, TTN, and FAT1 (Fig. 6B&C). Moreover, Fig. 6D demonstrates the occurrence of concurrent or independent mutations in the leading 25 frequently mutated genes. The high PAN.Score group demonstrated a significantly higher amount of concurrent gene modifications than the low PAN.Score group. RYR2 mutations frequently coexisted with TTN mutations in the high PAN.Score group. The list of mutant loci were NOTCH1 and FAT1; RYR2 and FAT4; PCDH15 and RYR2. In the low PAN.Score group, common co-mutations included TP53 and CDKN2A, along with RYR2 and TTN. By contrast, the high PAN.Score group revealed dense mutually exclusive gene alteration pairs, such as TP53-PIK3CA, whereas TP53-CASP8 pairs were discovered in the low PAN.Score group (Fig. 6D).

The correlation between PAN.Score and immune status in the TCGA-HNSCC dataset were examined using the ESTIMATE algorithm. Our results demonstrated that HNSCC patients with low PAN.Score scores had significantly higher ESTIMATE scores, immune scores, and stromal cells than HNSCC patients with high PAN.Score scores (Fig. 7A). The PAN.Score level in HNSCC patients indicates an inverse correlation with their immune status. To confirm this phenotype, we used the ssGSEA and TIMER algorithms individually to assess the frequency of immune infiltrating cell populations based on PAN.Score, tumor stage, tumor grade, gender, and age (Fig. 7B&C). Therefore, the heat map showed that many immune infiltrating cells were plentiful in HNSCC patients with high PAN.Score, including CD8 T cells, cytotoxic lymphocytes, NK cells, and neutrophils (Fig. 7B).

3.6. In TCGA cohorts with HNSCC, PAN.Score correlated with immune therapy

The GSVA heat map displayed pathways related to PAN.Score. Furthermore, it unveiled diverse pathways linked to NIFK, encompassing immune-related functions and tumor-related pathways from GO and KEGG. Significantly, increased NIFK levels exhibited a robust association with KEGG pathways that control the regulation of the cell cycle, DNA synthesis, and proteasome function. By contrast, reduced NIFK levels were associated with immune-related pathways, including differentiation of natural killer cells, proliferation of leukocytes, and immune response (Fig. 8A). Further examination suggested decreased levels of PAN.Score were relevant to immune checkpoint levels in TCGA (Fig. 8B). Furthermore, a significant association was noted between the expression of CD27 and specific treatments (such as sapitinib, lbrutinib, and sepantronium bromide), indicating low PAN.Score group reacted better to targeted therapies (see Fig. 8C). Therefore, these findings suggest that PAN.Score has significant promise as a prognostic marker for HNSCC patients.

3.7. The PAN.Score gene CD27 plays a key role in HNSCC cells

We examined the function of CD27 in HNSCC by using shRNA lentiviruses containing GFP to suppress CD27 expression in SCC15 cells. Cells that underwent transfection were chosen using puromycin, and the reduction in CD27 expression was assessed using RT-PCR. Fluorescence microscopy and RT-PCR were used to validate the expression of CD27 (Fig. 9A&B). Functional assays revealed that reducing CD27 expression in SCC15 cells resulted in a decline in cell proliferation (MTT, Fig. 9E), colony formation (Plate cloning, Fig. 9C&D), and migration (scratch migration, Fig. 9F&G). The results indicate that the gene CD2 has a significant effect on HNSCC cells.

4. Discussion

HNSCC patients at intermediate to advanced stages, renowned for their hostile and spreading characteristics, frequently encounter a bleak outlook primarily because of drug resistance and numerous additional elements [5]. PANoptosis—a novel mode of programmed cell demise—is an inflammatory cell death controlled by the PANoptosome complex. PANoptosis involves the combination and cooperation of various programmed cell death pathways [18], including pyroptosis, apoptosis, and/or necroptosis. Nevertheless,

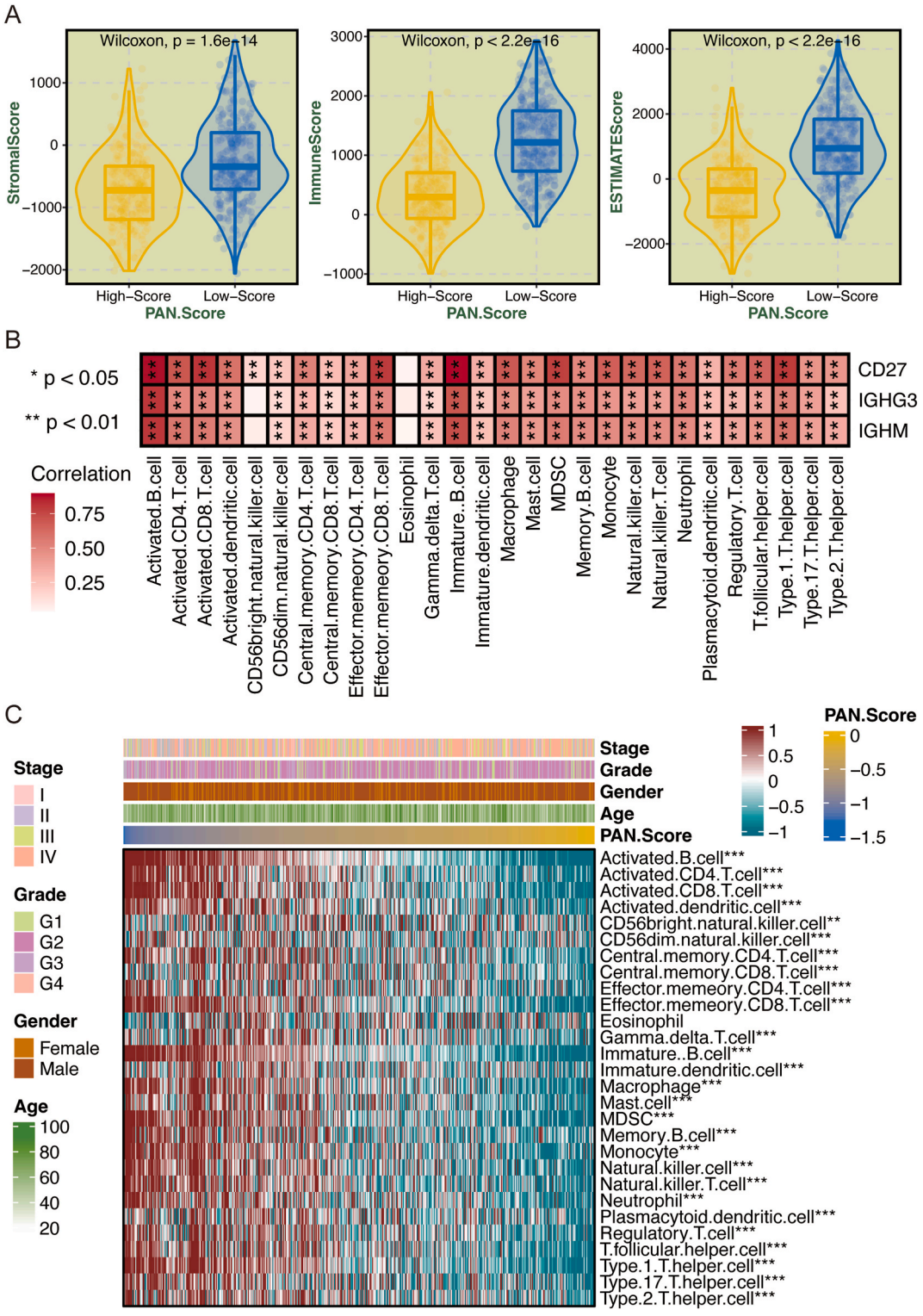

Fig. 7. Relationship between PAN.Score and immunization in the TCGA-HNSCC cohort. (A) Difference in ESTIMATE between high and low PAN. Score groups. (B) Association of 28 immune cell infiltrates (ssGSEA) with the 3 genes in PAN.Score. (C) Heat map showing the association of 28 immune cell infiltrates (ssGSEA) with PAN.Score. *p < 0.05; **p < 0.01, ***p < 0.005.

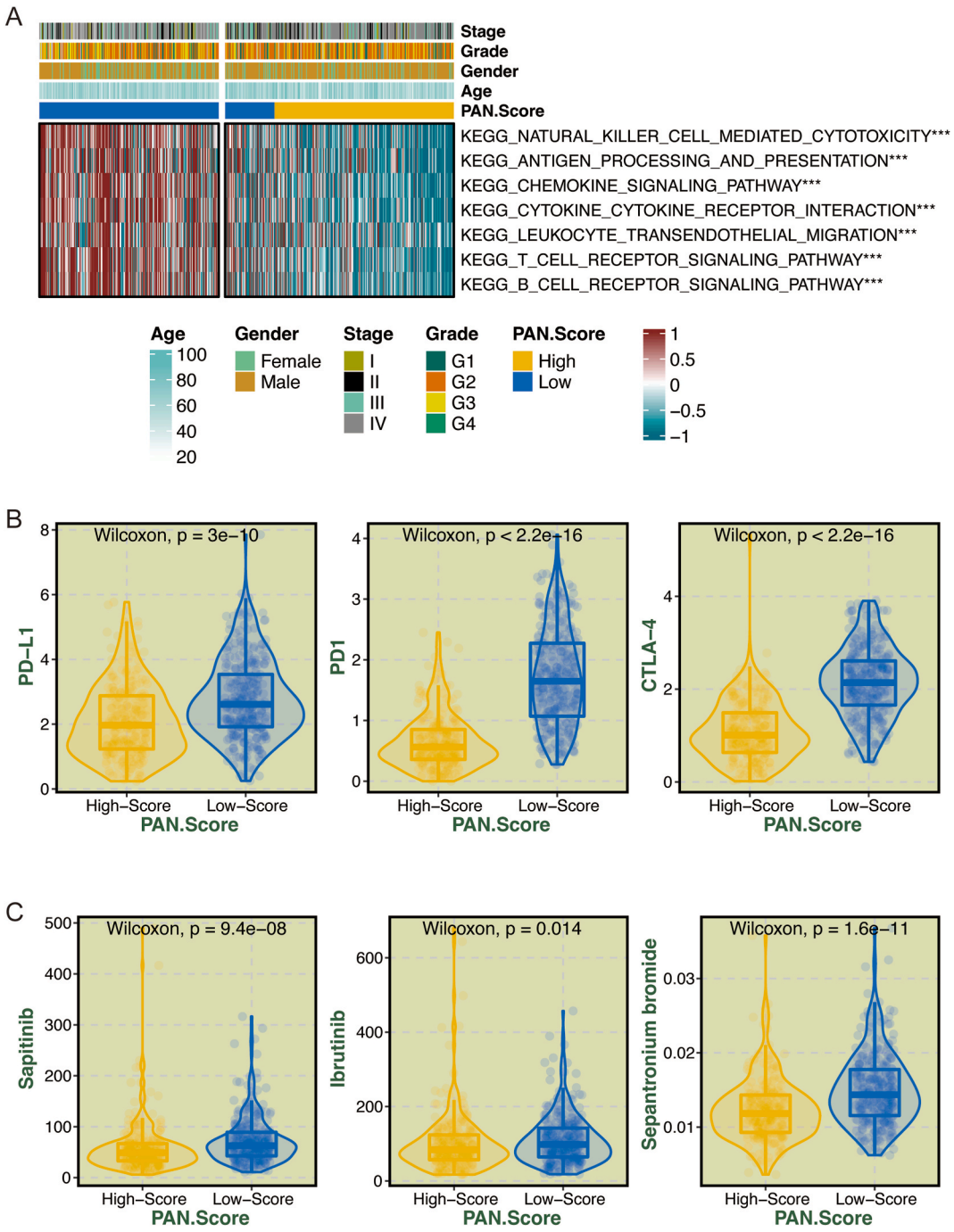

Fig. 8. Immunotherapy and chemotherapy involved in PAN.Score in TCGA head and neck cancer. (A) GSVA heat map of immune-related pathways associated with PAN.Score in TCGA. (B) Relationship between PAN.Score and 3 classical immune checkpoints in TCGA. (C) Box plot of estimated IC50 of several chemotherapeutic agents in TCGA in high PAN.Score and low PAN.Score groups. ***p < 0.005.

the association between PANoptosis and HNSCC remains inadequately investigated, and specifically, the precise functions of PARGs in HNSCC remain undisclosed. To reveal the importance of PANoptosis in HNSCC, we sought to establish a correlation between PANoptosis and the prognosis of HNSCC patients. Furthermore, triggering PANoptosis can prompt tumor cells to release cytokines that stimulate an immune response [35], which activates the body's immune system to target and eliminate tumor cells, presenting a new and promising treatment approach for HNSCC.

By inducing PANoptosis in cancer cells, immunotherapy methods can simultaneously activate multiple cell death pathways, thereby enhancing immunogenic signals and facilitating the activation of immune cells. This process enhances the presentation of

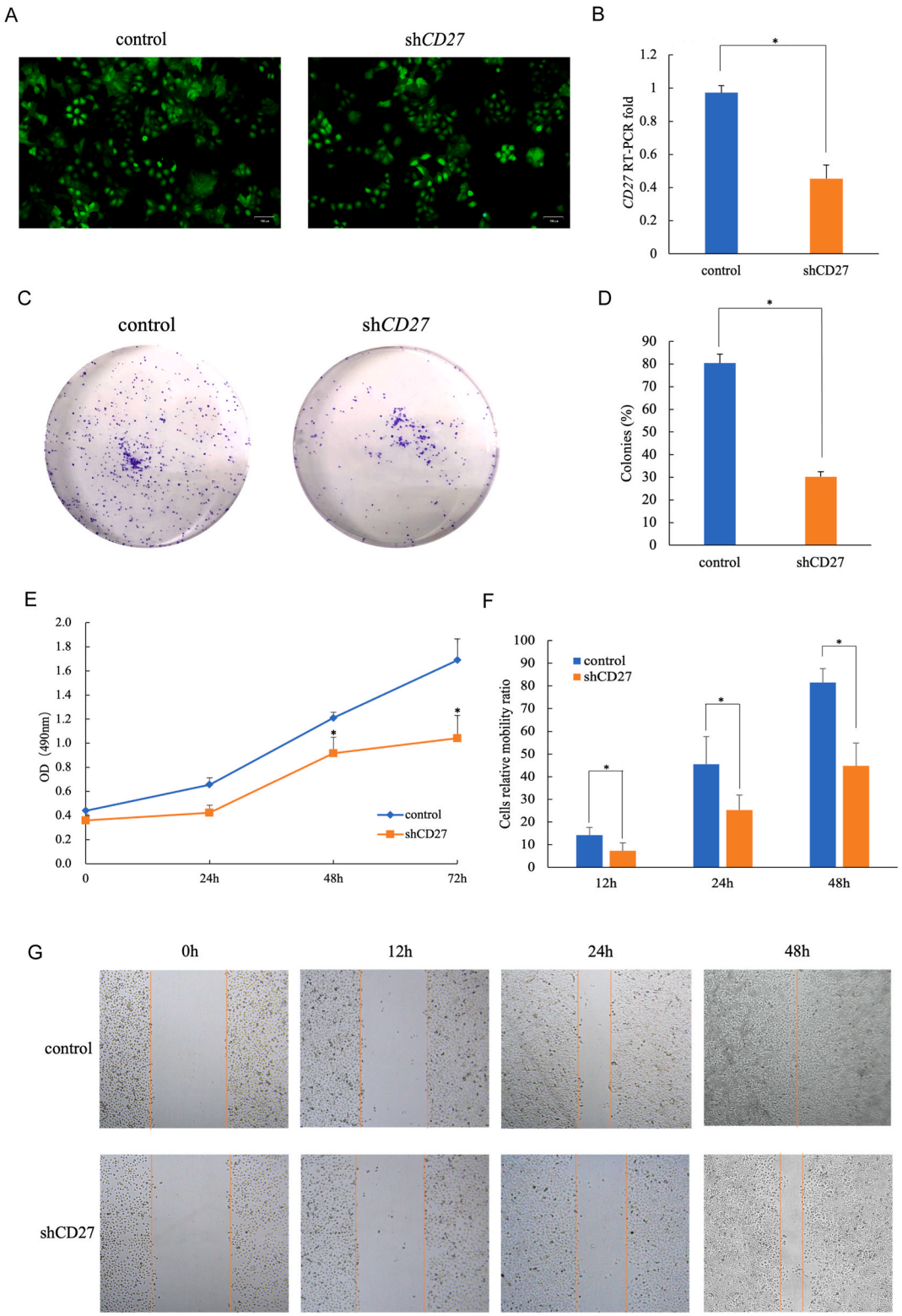

Fig. 9. The PAN.Score gene CD27 plays a key role in SCC15 cells. (A)Stable transfection of lentivirus with control and shCD27 in SCC15 cells is indicated by green fluorescence (200 ×). (B) Expression of CD27 assessed by RT-PCR. (C–D) Plate cloning assay and its quantitative analysis in SCC15 cells. (E) MTT assay in SCC15 cells. (F–G) Scratch migration assay(G) and its quantitative analysis(F) in SCC15 cells (4 ×). *$p < 0.05$. Each experiment was performed three times independently.

tumor antigens, facilitating the immune system's recognition of cancer cells [36,37]. The release of danger-associated molecular patterns and cytokines during PANoptosis serves as a stimulus for dendritic cells and antigen-presenting cells, leading to the maturation and activation of adaptive immune responses [38]. Furthermore, the interplay between different cell death pathways in PANoptosis can yield synergistic effects on immune cell activation. For instance, initiating necroptosis may lead to the liberation of ATP, functioning as a warning sign promoting dendritic cell activation [39]. Following the activation of pyroptosis and the subsequent release of pro-inflammatory cytokines, there is an additional contribution to the recruitment and activation of immune cells. The pursuit of PANoptosis in cancer immunotherapy presents hopeful opportunities for the advancement of novel therapeutic approaches. Through modulation of the cellular signaling pathways associated with PANoptosis, researchers can potentially boost the immunogenicity of cancer cells, enhance the presentation of antigens, and strengthen the immune responses against tumors. Nevertheless, it is essential to recognize that the exact processes and treatment strategies aimed at PANoptosis in cancer are under investigation, requiring additional research to fully grasp its possibilities and constraints in cancer immunotherapy.

PANoptosis is a coordinated process in which any of the three programmed cell death pathways can work together and cooperate at different times depending on the stimuli in the tumor microenvironment [40]. In patients undergoing immunotherapy, if the apoptosis process is obstructed in cancer cells, alternative programmed cell death pathways, such as thermal apoptosis or necrosis, may be activated to eradicate the cancer cells. Malireddi et al. reported that PANoptosis in cancer cells could trigger strong immune responses against cancer, resulting in improved efficacy of immunotherapy, even in cancers unresponsive to immune checkpoint inhibitors [41]. By identifying PANoptosis as a vital process for inhibiting tumor growth, the collaboration between TNF-α and IFN-γ has been recognized and could potentially be targeted for innovative treatments [16].

The regulatory mode of PANoptosis has not yet been investigated. The present study examined the expression of PAN-related genes in HNSCC and identified two separate PANoptosis patterns—PAN cluster 1 and PAN cluster 2 (Figs. 1 and 2). The prognostic, predictive ability of the PAN.Score, developed with CD27, IGHG3, and IGHM, three PAN genes linked to prognosis, was thoroughly confirmed in three distinct cohorts (GSE41613, GSE42743, and GSE65858). Moreover, PAN.Score demonstrates effective prediction of immunotherapy outcomes. The lower PAN.Score group showed a better reaction to chemotherapy than the higher PAN.Score group. Moreover, patients with gastric cancer [42,43], or colon cancer [22] might experience PANoptosis, making immunotherapy potentially advantageous for them.

We presented a study on the characteristics of PANoptosis in HNSCC, including clinical, molecular, and immunological aspects. With the advancement of our comprehension regarding PANoptosis, we anticipate an increase in research uncovering the potential mechanisms of PANoptosis in relation to cancer. Naturally, there exist certain constraints within the research. Initially, the data for analysis were sourced from publicly available databases, seldom comprising randomly selected potential samples. Furthermore, the molecular biology experiments conducted so far have only obtained initial validation. Nevertheless, no practical tests of relevance have been conducted. In conclusion, the clinical features provided are insufficient; thus, it is necessary to assess our findings using real-life clinical cases.

Our findings indicate that PANoptosis pathways may play a critical role in shaping the immune response in HNSCC. Specifically, the modulation of these pathways could either enhance the efficacy of immunotherapies by promoting an immune-activating tumor microenvironment or conversely, lead to resistance by fostering immune suppression. Understanding these mechanisms offers promising avenues for optimizing immunotherapy in HNSCC patients.

In our survival analysis using the Cox proportional hazards model, we focused on assessing the impact of individual PANoptosis-related genes on patient survival. The fitting of the Cox model allowed us to estimate hazard ratios, providing insights into the relative risk of death associated with each gene. To evaluate the performance of our model, we employed Harrell's concordance index and conducted log-rank tests. These metrics were instrumental in demonstrating the model's effectiveness and reliability in predicting survival outcomes in our study population. Additionally, to aid in the interpretation of our findings, we included Kaplan-Meier curves and hazard ratio plots. These visual representations not only illustrate the survival probabilities over time but also effectively communicate the influence of specific PRGs on survival outcomes.

The current landscape of immunotherapy in HNSCC primarily revolves around checkpoint inhibitors, such as PD-1/PD-L1 and CTLA-4 antagonists. These therapies have revolutionized treatment, yet they are effective in only a subset of patients. Herein lies the distinct potential of targeting PANoptosis in HNSCC. Unlike checkpoint inhibitors that predominantly modulate the immune system's ability to recognize and attack cancer cells, PANoptosis-targeted therapies could fundamentally alter the tumor microenvironment. By inducing a form of cell death that potentially releases more tumor antigens and pro-inflammatory cytokines, PANoptosis might enhance the overall immunogenicity of HNSCC tumors. This could, in theory, render previously unresponsive tumors more susceptible to existing immunotherapies, such as checkpoint inhibitors.

To summarize, we have discovered two separate PANoptosis patterns that could offer fresh perspectives on the correlation between PANoptosis and the clinical, molecular, and immunological characteristics of HNSCC. Furthermore, we developed a PAN.Score that has the potential to provide a more precise prognosis for HNSCC patients and can serve as a valuable tool in guiding clinical interventions, ultimately enhancing the effectiveness of personalized treatment approaches for HNSCC patients.

Although our study provides significant insights into the prognostic value of PAN.Score in HNSCC, its broader implications warrant further discussion. The identification of specific PANoptosis-related genes that significantly influence patient outcomes not only advances our understanding of HNSCC pathophysiology but also opens new avenues for research. Future studies could focus on the mechanistic role of these genes in HNSCC progression and response to therapy, which may lead to the development of targeted therapeutic strategies. Furthermore, the clinical implications of our findings are substantial. The integration of PAN.Score into clinical practice could revolutionize the prognostic assessment and treatment planning for HNSCC patients. It offers a potential tool for clinicians to more accurately predict patient outcomes and tailor treatment approaches accordingly. The use of PAN.Score could be

particularly impactful in the realm of personalized medicine, where individualized treatment decisions are paramount. Therefore, our study not only contributes to the scientific understanding of HNSCC but also paves the way for improved patient management strategies.

Our study highlights the prognostic significance of PAN.Score in HNSCC, but its potential clinical applications extend further. Integrating PAN.Score into current clinical workflows could significantly enhance patient management in HNSCC. For instance, by incorporating PAN.Score into routine diagnostic procedures, clinicians could more accurately assess disease prognosis, guiding more personalized treatment plans. This approach aligns with the principles of personalized medicine, where treatment decisions are tailored to individual patient profiles. We suggest future studies to explore the feasibility and practicality of implementing PAN.Score in clinical settings, examining its impact on treatment outcomes and patient quality of life. As we chart the course for future research, it is imperative to consider several key directions. Firstly, further validation studies are needed to confirm our findings across diverse patient populations and clinical settings. Additionally, investigating the molecular mechanisms underlying PAN.Score could reveal new therapeutic targets in HNSCC. Moreover, the potential applicability of our research to other cancer types presents an exciting avenue for extending the impact of our findings, potentially contributing to a broader understanding of cancer biology and treatment.

Ethics approval and consent to participate

Not applicable.

Consent for publication

All the authors read and approved the final version of the manuscript.

Availability of data and materials

The datasets presented in this study are available online. The TCGA and GEO (GSE4161), GSE4274, and GSE65858 provided comprehensive clinicopathological annotation and genomic data for HNSCC.

Data availability statement

No data been deposited into a publicly available repository. Data will be made available on request.

CRediT authorship contribution statement

Feng Gao: Writing – review & editing, Writing – original draft, Validation, Methodology, Investigation, Funding acquisition, Conceptualization. **Minghuan Zhang:** Validation, Methodology, Investigation, Data curation. **Zhenguang Ying:** Software, Project administration, Methodology, Data curation. **Wanqiu Li:** Resources, Investigation, Formal analysis. **Desheng Lu:** Validation, Supervision. **Xia Wang:** Writing – review & editing, Validation, Supervision, Investigation, Funding acquisition, Formal analysis, Conceptualization. **Ou Sha:** Writing – review & editing, Validation, Supervision, Funding acquisition, Formal analysis, Data curation, Conceptualization.

Declaration of competing interest

The authors declare that they have no known competing financial interests or personal relationships that could have appeared to influence the work reported in this paper.

Acknowledgements

This study was financially supported by the Key Fundamental Research Fund of Science and Technology Foundation of Shenzhen City (Grant No. JCYJ20210324094005015 and JCYJ20220818095811026), Guangdong Natural Science Foundation General Program (Grant No. 2023A1515010615) and Shenzhen Science and Technology Innovation Commission stable support project (Grant No. 20220810174028001).

Appendix A. Supplementary data

Supplementary data to this article can be found online at https://doi.org/10.1016/j.heliyon.2024.e27162.

References

[1] V. Van den Bossche, H. Zaryouh, M. Vara-Messler, J. Vignau, J.-P. Machiels, A. Wouters, S. Schmitz, C. Corbet, Microenvironment-driven intratumoral heterogeneity in head and neck cancers: clinical challenges and opportunities for precision medicine, Drug Resist. Updates 60 (2022) 100806, https://doi.org/10.1016/j.drup.2022.100806.

[2] L.-L. Bu, H.-Q. Wang, Y. Pan, L. Chen, H. Wu, X. Wu, C. Zhao, L. Rao, B. Liu, Z.-J. Sun, Gelatinase-sensitive nanoparticles loaded with photosensitizer and STAT3 inhibitor for cancer photothermal therapy and immunotherapy, J. Nanobiotechnol. 19 (2021) 379, https://doi.org/10.1186/s12951-021-01125-7.

[3] M. Yang, Q. Luo, X. Chen, F. Chen, Bitter melon derived extracellular vesicles enhance the therapeutic effects and reduce the drug resistance of 5-fluorouracil on oral squamous cell carcinoma, J. Nanobiotechnol. 19 (2021) 259, https://doi.org/10.1186/s12951-021-00995-1.

[4] L. Liu, J. Chen, X. Cai, Z. Yao, J. Huang, Progress in targeted therapeutic drugs for oral squamous cell carcinoma, Surgical Oncology 31 (2019) 90–97, https://doi.org/10.1016/j.suronc.2019.09.001.

[5] C. Borel, A.C. Jung, M. Burgy, Immunotherapy Breakthroughs in the treatment of recurrent or metastatic head and neck squamous cell carcinoma, Cancers 12 (2020) 2691, https://doi.org/10.3390/cancers12092691.

[6] S. Park, C.G. Kim, D. Kim, M.H. Hong, E.C. Choi, S.-H. Kim, Y.M. Park, J. Kim, S.O. Yoon, G. Kim, S. Shin, K. Kim, Y.W. Koh, S.-J. Ha, H.R. Kim, Disproportional enrichment of FoxP3(+) CD4(+) regulatory T cells shapes a suppressive tumour microenvironment in head and neck squamous cell carcinoma, Clin. Transl. Med. 12 (2022) e753, https://doi.org/10.1002/ctm2.753.

[7] H. Zhang, Z. Dai, W. Wu, Z. Wang, N. Zhang, L. Zhang, W.-J. Zeng, Z. Liu, Q. Cheng, Regulatory mechanisms of immune checkpoints PD-L1 and CTLA-4 in cancer, J. Exp. Clin. Cancer Res. 40 (2021) 184, https://doi.org/10.1186/s13046-021-01987-7.

[8] S.L. Topalian, F.S. Hodi, J.R. Brahmer, S.N. Gettinger, D.C. Smith, D.F. McDermott, J.D. Powderly, R.D. Carvajal, J.A. Sosman, M.B. Atkins, P.D. Leming, D. R. Spigel, S.J. Antonia, L. Horn, C.G. Drake, D.M. Pardoll, L. Chen, W.H. Sharfman, R.A. Anders, J.M. Taube, T.L. McMiller, H. Xu, A.J. Korman, M. Jure-Kunkel, S. Agrawal, D. McDonald, G.D. Kollia, A. Gupta, J.M. Wigginton, M. Sznol, Safety, activity, and immune correlates of anti–PD-1 antibody in cancer, N. Engl. J. Med. 366 (2012) 2443–2454, https://doi.org/10.1056/NEJMoa1200690.

[9] Y. Huang, P. Zhang, Immunogenomic alterations of head and neck squamous cell carcinomas stratified by smoking status, Clin. Transl. Med. 11 (2021) 1–5, https://doi.org/10.1002/ctm2.599.

[10] Y. Xue, X. Jiang, J. Wang, Y. Zong, Z. Yuan, S. Miao, X. Mao, Effect of regulatory cell death on the occurrence and development of head and neck squamous cell carcinoma, Biomark. Res. 11 (2023) 2, https://doi.org/10.1186/s40364-022-00433-w.

[11] J.-F. Lin, P.-S. Hu, Y.-Y. Wang, Y.-T. Tan, K. Yu, K. Liao, Q.-N. Wu, T. Li, Q. Meng, J.-Z. Lin, Z.-X. Liu, H.-Y. Pu, H.-Q. Ju, R.-H. Xu, M.-Z. Qiu, Phosphorylated NFS1 weakens oxaliplatin-based chemosensitivity of colorectal cancer by preventing PANoptosis, Signal Transduct. Targeted Ther. 7 (2022) 54, https://doi.org/10.1038/s41392-022-00889-0.

[12] Y. Cai, X. Chen, T. Lu, X. Fang, M. Ding, Z. Yu, S. Hu, J. Liu, X. Zhou, X. Wang, Activation of STING by SAMHD1 deficiency promotes PANoptosis and enhances efficacy of PD-L1 blockade in diffuse large B-cell lymphoma, Int. J. Biol. Sci. 19 (2023) 4627–4643, https://doi.org/10.7150/ijbs.85236.

[13] F. Song, C.-G. Wang, J.-Z. Mao, T.-L. Wang, X.-L. Liang, C.-W. Hu, Y. Zhang, L. Han, Z. Chen, PANoptosis-based molecular subtyping and HPAN-index predicts therapeutic response and survival in hepatocellular carcinoma, Front. Immunol. 14 (2023) 1197152, https://doi.org/10.3389/fimmu.2023.1197152.

[14] R. Karki, B.R. Sharma, E. Lee, B. Banoth, R.K.S. Malireddi, P. Samir, S. Tuladhar, H. Mummareddy, A.R. Burton, P. Vogel, T.-D. Kanneganti, Interferon regulatory factor 1 regulates PANoptosis to prevent colorectal cancer, JCI Insight 5 (2020) 136720, https://doi.org/10.1172/jci.insight.136720.

[15] R. Karki, B. Sundaram, B.R. Sharma, S. Lee, R.K.S. Malireddi, L.N. Nguyen, S. Christgen, M. Zheng, Y. Wang, P. Samir, G. Neale, P. Vogel, T.-D. Kanneganti, ADAR1 restricts ZBP1-mediated immune response and PANoptosis to promote tumorigenesis, Cell Rep. 37 (2021) 109858, https://doi.org/10.1016/j.celrep.2021.109858.

[16] R.K.S. Malireddi, R. Karki, B. Sundaram, B. Kancharana, S. Lee, P. Samir, T.-D. Kanneganti, Inflammatory cell death, PANoptosis, mediated by cytokines in diverse cancer lineages inhibits tumor growth, ImmunoHorizons 5 (2021) 568–580, https://doi.org/10.4049/immunohorizons.2100059.

[17] X. Yi, J. Li, X. Zheng, H. Xu, D. Liao, T. Zhang, Q. Wei, H. Li, J. Peng, J. Ai, Construction of PANoptosis signature: novel target discovery for prostate cancer immunotherapy, Mol. Ther. Nucleic Acids 33 (2023) 376–390, https://doi.org/10.1016/j.omtn.2023.07.010.

[18] P. Samir, R.K.S. Malireddi, T.-D. Kanneganti, The PANoptosome: a deadly protein complex driving pyroptosis, apoptosis, and necroptosis (PANoptosis), Front. Cell. Infect. Microbiol. 10 (2020) 238, https://doi.org/10.3389/fcimb.2020.00238.

[19] A. Blum, P. Wang, J.C. Zenklusen, SnapShot: TCGA-analyzed tumors, Cell 173 (2018) 530, https://doi.org/10.1016/j.cell.2018.03.059.

[20] T. Barrett, S.E. Wilhite, P. Ledoux, C. Evangelista, I.F. Kim, M. Tomashevsky, K.A. Marshall, K.H. Phillippy, P.M. Sherman, M. Holko, A. Yefanov, H. Lee, N. Zhang, C.L. Robertson, N. Serova, S. Davis, A. Soboleva, NCBI GEO: archive for functional genomics data sets—update, Nucleic Acids Res. 41 (2012) D991–D995, https://doi.org/10.1093/nar/gks1193.

[21] Z. Wang, X. Wang, N. Zhang, H. Zhang, Z. Dai, M. Zhang, S. Feng, Q. Cheng, Pentraxin 3 promotes glioblastoma progression by negative regulating cells autophagy, Front. Cell Dev. Biol. 8 (2020) 795, https://doi.org/10.3389/fcell.2020.00795.

[22] X. Wang, R. Sun, S. Chan, L. Meng, Y. Xu, X. Zuo, Z. Wang, X. Hu, Q. Han, L. Dai, T. Bai, Z. Yu, M. Wang, W. Yang, H. Zhang, W. Chen, PANoptosis-based molecular clustering and prognostic signature predicts patient survival and immune landscape in colon cancer, Front. Genet. 13 (2022) 955355, https://doi.org/10.3389/fgene.2022.955355.

[23] M.D. Wilkerson, D.N. Hayes, ConsensusClusterPlus: a class discovery tool with confidence assessments and item tracking, Bioinformatics 26 (2010) 1572–1573, https://doi.org/10.1093/bioinformatics/btq170.

[24] X.-N. Wu, D. Su, Y.-D. Mei, M.-Q. Xu, H. Zhang, Z.-Y. Wang, L.-L. Li, L. Peng, J.-Y. Jiang, J.-Y. Yang, D.-J. Li, H. Cao, Z.-W. Xia, W.-J. Zeng, Q. Cheng, N. Zhang, Identified lung adenocarcinoma metabolic phenotypes and their association with tumor immune microenvironment, Cancer Immunol. Immunother. 70 (2021) 2835–2850, https://doi.org/10.1007/s00262-021-02896-6.

[25] N. Zhang, H. Zhang, W. Wu, R. Zhou, S. Li, Z. Wang, Z. Dai, L. Zhang, F. Liu, Z. Liu, J. Zhang, P. Luo, Z. Liu, Q. Cheng, Machine learning-based identification of tumor-infiltrating immune cell-associated lncRNAs for improving outcomes and immunotherapy responses in patients with low-grade glioma, Theranostics 12 (2022) 5931–5948, https://doi.org/10.7150/thno.74281.

[26] X. Li, Z. Dai, X. Wu, N. Zhang, H. Zhang, Z. Wang, X. Zhang, X. Liang, P. Luo, J. Zhang, Z. Liu, Y. Zhou, Q. Cheng, R. Chang, The comprehensive analysis identified an autophagy signature for the prognosis and the immunotherapy efficiency prediction in lung adenocarcinoma, Front. Immunol. 13 (2022) 749241, https://doi.org/10.3389/fimmu.2022.749241.

[27] A. Liberzon, C. Birger, H. Thorvaldsdóttir, M. Ghandi, J.P. Mesirov, P. Tamayo, The molecular signatures database hallmark gene set collection, Cell Systems 1 (2015) 417–425, https://doi.org/10.1016/j.cels.2015.12.004.

[28] T. Wu, E. Hu, S. Xu, M. Chen, P. Guo, Z. Dai, T. Feng, L. Zhou, W. Tang, L. Zhan, X. Fu, S. Liu, X. Bo, G. Yu, clusterProfiler 4.0: a universal enrichment tool for interpreting omics data, Innovation 2 (2021) 100141, https://doi.org/10.1016/j.xinn.2021.100141.

[29] S. Hänzelmann, R. Castelo, J. Guinney, GSVA: gene set variation analysis for microarray and RNA-Seq data, BMC Bioinf. 14 (2013) 7, https://doi.org/10.1186/1471-2105-14-7.

[30] S. Li, N. Zhang, S. Liu, H. Zhang, J. Liu, Y. Qi, Q. Zhang, X. Li, ITGA5 is a novel oncogenic biomarker and correlates with tumor immune microenvironment in gliomas, Front. Oncol. 12 (2022) 844144, https://doi.org/10.3389/fonc.2022.844144.

[31] Z. Zhu, Z. Ying, M. Zeng, Q. Zhang, G. Liao, Y. Liang, C. Li, C. Zhang, X. Wang, W. Jiang, P. Luan, O. Sha, Trichosanthin cooperates with Granzyme B to restrain tumor formation in tongue squamous cell carcinoma, BMC Complement Med Ther 21 (2021) 88, https://doi.org/10.1186/s12906-021-03266-6.

[32] J. Wen, P. Yin, Y. Su, F. Gao, Y. Wu, W. Zhang, P. Chi, J. Chen, X. Zhang, Knockdown of HMGB1 inhibits the crosstalk between oral squamous cell carcinoma cells and tumor-associated macrophages, Int. Immunopharm. 119 (2023) 110259, https://doi.org/10.1016/j.intimp.2023.110259.

[33] Y. Zou, J. Xie, S. Zheng, W. Liu, Y. Tang, W. Tian, X. Deng, L. Wu, Y. Zhang, C.-W. Wong, D. Tan, Q. Liu, X. Xie, Leveraging diverse cell-death patterns to predict the prognosis and drug sensitivity of triple-negative breast cancer patients after surgery, Int. J. Surg. 107 (2022) 106936, https://doi.org/10.1016/j.ijsu.2022.106936.

[34] J. Zhang, Z. Wang, X. Zhang, Z. Dai, W. Zhi-Peng, J. Yu, Y. Peng, W. Wu, N. Zhang, P. Luo, J. Zhang, Z. Liu, S. Feng, H. Zhang, Q. Cheng, Large-scale single-cell and bulk sequencing analyses reveal the prognostic value and immune aspects of CD147 in pan-cancer, Front. Immunol. 13 (2022) 810471, https://doi.org/10.3389/fimmu.2022.810471.
[35] W. Liu, C. Qu, X. Wang, Comprehensive analysis of the role of immune-related PANoptosis lncRNA model in renal clear cell carcinoma based on RNA transcriptome and single-cell sequencing, Oncol. Res. 31 (2023) 543–567, https://doi.org/10.32604/or.2023.029563.
[36] K. Pang, Z.-D. Shi, L.-Y. Wei, Y. Dong, Y.-Y. Ma, W. Wang, G.-Y. Wang, M.-Y. Cao, J.-J. Dong, Y.-A. Chen, P. Zhang, L. Hao, H. Xu, D. Pan, Z.-S. Chen, C.-H. Han, Research progress of therapeutic effects and drug resistance of immunotherapy based on PD-1/PD-L1 blockade, Drug Resist. Updates 66 (2023) 100907, https://doi.org/10.1016/j.drup.2022.100907.
[37] B. Yan, S. Wang, C. Liu, N. Wen, H. Li, Y. Zhang, H. Wang, Z. Xi, Y. Lv, H. Fan, X. Liu, Engineering magnetic nano-manipulators for boosting cancer immunotherapy, J. Nanobiotechnol. 20 (2022) 547, https://doi.org/10.1186/s12951-022-01760-8.
[38] X. Xu, Y. Wei, J. Pang, Z. Wei, L. Wang, Q. Chen, Z. Wang, Y. Zhang, K. Chen, Y. Peng, Z. Zhang, J. Liu, Y. Zhang, Z.-B. Jin, Q. Liang, Time-course transcriptomic analysis reveals the crucial roles of PANoptosis in fungal keratitis, Invest. Ophthalmol. Vis. Sci. 64 (2023) 6, https://doi.org/10.1167/iovs.64.3.6.
[39] R. Luo, K. Onyshchenko, L. Wang, S. Gaedicke, A.-L. Grosu, E. Firat, G. Niedermann, Necroptosis-dependent immunogenicity of cisplatin: implications for enhancing the radiation-induced abscopal effect, Clin. Cancer Res. 29 (2023) 667–683, https://doi.org/10.1158/1078-0432.CCR-22-1591.
[40] N. Pandian, T.-D. Kanneganti, PANoptosis: a unique innate immune inflammatory cell death modality, J. Immunol. 209 (2022) 1625–1633, https://doi.org/10.4049/jimmunol.2200508.
[41] R. Tang, J. Xu, B. Zhang, J. Liu, C. Liang, J. Hua, Q. Meng, X. Yu, S. Shi, Ferroptosis, necroptosis, and pyroptosis in anticancer immunity, J. Hematol. Oncol. 13 (2020) 110, https://doi.org/10.1186/s13045-020-00946-7.
[42] H. Pan, J. Pan, P. Li, J. Gao, Characterization of PANoptosis patterns predicts survival and immunotherapy response in gastric cancer, Clin. Immunol. 238 (2022) 109019, https://doi.org/10.1016/j.clim.2022.109019.
[43] S.T. Kim, R. Cristescu, A.J. Bass, K.-M. Kim, J.I. Odegaard, K. Kim, X.Q. Liu, X. Sher, H. Jung, M. Lee, S. Lee, S.H. Park, J.O. Park, Y.S. Park, H.Y. Lim, H. Lee, M. Choi, A. Talasaz, P.S. Kang, J. Cheng, A. Loboda, J. Lee, W.K. Kang, Comprehensive molecular characterization of clinical responses to PD-1 inhibition in metastatic gastric cancer, Nat Med 24 (2018) 1449–1458, https://doi.org/10.1038/s41591-018-0101-z.